Physics in Nuclear Medicine

Second Edition

James A. Sorenson, Ph.D.
Director, Medical Physics
Professor of Radiology
Department of Radiology
University of Utah Medical Center
Salt Lake City, Utah

Michael E. Phelps, Ph.D.
Jennifer Jones Simon Professor
Chief, Division of Nuclear Medicine and Biophysics
Department of Radiological Sciences
UCLA School of Medicine
Chief, Laboratory of Nuclear Medicine
Laboratory of Biomedical and Environmental Sciences, UCLA
Los Angeles, California

W.B. SAUNDERS COMPANY
Harcourt Brace Jovanovich, Inc.
Philadelphia London Toronto Montreal Sydney Tokyo

16
The Anger Camera: Performance Characteristics

B. DESIGN AND PERFORMANCE CHARACTERISTICS OF PARALLEL-HOLE COLLIMATORS

1. Basic Limitations in Collimator Performance

The collimator is a "weak link" for the performance of an Anger camera system, as indeed it is in any nuclear medicine imaging system employing the principles of *absorptive collimation*. *Collimator efficiency*, defined as the fraction of γ rays striking the collimator that actually pass through it to project the γ-ray image onto the detector, is typically only a few percent or less. *Collimator resolution*, which refers to the sharpness or detail of the γ-ray image projected onto the detector, also is rather poor, generally worse than the intrinsic resolution of the camera detector and electronics.

Because it is a limiting factor in camera system performance, it is important that the collimator be designed carefully. Poor design can result only in poorer overall performance. Design considerations for parallel-hole collimators will be discussed in this section. Design characteristics for converging and diverging collimators are similar to those of the parallel-hole type. Design characteristics of pinhole collimators will not be discussed in detail here but are described in references listed at the end of the chapter. The analysis to be presented for parallel-hole collimators

is similar to that presented by Anger in reference 1, which may be consulted for a more detailed discussion.

2. Septal Thickness

A primary consideration in collimator design is to ensure that *septal penetration* by γ rays crossing from one collimator hole into another is negligibly small. This is essential if an accurate γ-ray image is to be projected by the collimator onto the camera detector. No thickness of septal material is sufficient to stop *all* γ rays, so the usual criteria is to accept some reasonably small level of septal penetration, e.g., ~5 percent.

The required septal thickness may be determined by analysis of Figure 16-11. The shortest path length for γ rays to travel from one hole to the next is w. Septal thickness t is related to w, and to the length l and diameter d of the collimator holes, by[1]

$$t = 2dw/(l - w) \tag{16-1}$$

If septal penetration is to be less than 5 percent, the transmission factor for the thickness w must be

$$e^{-\mu w} \lesssim 0.05 \tag{16-2}$$

where μ is the linear attenuation coefficient of the septal material. Since $e^{-3} \sim 0.05$, this implies

$$\mu w \gtrsim 3 \tag{16-3}$$

$$w > 3/\mu \tag{16-4}$$

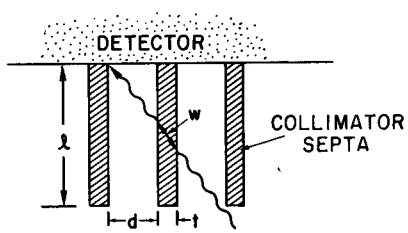

Fig. 16-11. Minimum path length w for a γ ray passing through the collimator septa from one hole to the next depends on length l and diameter d of the collimator holes and on septal thicknesses t.

and thus

$$t \gtrsim \frac{6d/\mu}{l - (3/\mu)} \tag{16-5}$$

It is desirable that septal thickness t be as small as possible so that the collimator septa obstruct the smallest possible area of detector surface and collimator efficiency is maximized. This objective is realized by using a material with a large value of μ for the collimator septa. Materials of high atomic number Z and high density ρ are preferred. Lead ($Z = 82$, $\rho = 11.34$ g/cm^3) is the material of choice for reasons of cost and availability; however, other materials, including tantalum ($Z = 73$, $\rho = 16.6$ g/cm^3), tungsten ($Z = 74$, $\rho = 19.4$ g/cm^3), and even gold ($Z = 79$, $\rho = 19.3$ g/cm^3) have been employed in experimental applications.

Attenuation coefficients of heavy elements depend strongly on γ-ray energy in the nuclear medicine energy range (Chapter 9, Section B.1). Thus the required septal thickness also depends strongly on the γ-ray energy for which the collimator is designed to be used. Commercially available collimators are categorized according to the maximum γ-ray energy for which their septal thickness is considered to be adequate. *Low-energy collimators* generally have an upper limit of about 150 keV and *medium-energy collimators* about 400 keV. High-energy collimators (e.g., 1 MeV) are not available commercially except by special order.

Example 16-1.

Calculate the septal thickness required for low-energy (150 keV) and medium-energy (400 keV) lead collimators having hole diameters 0.25 cm and lengths 2.5 cm.

Answer.

The linear attenuation coefficient of lead at 150 keV is $\mu_l = 1.89$ cm^2/g $\times$ 11.34 g/cm^3 = 21.43 cm^{-1} and at 400 keV is $\mu_l = 0.22$ cm^2/g $\times$ 11.34 g/cm^3 = 2.49 cm^{-1} (Appendix D). Therefore from Equation 16-5 for the low-energy collimator

$$t \gtrsim \frac{6 \times 0.25/21.43}{2.5 - \dfrac{3}{21.43}}$$

$$\gtrsim 0.030 \text{ cm}$$

and for the medium-energy collimator

$$t \gtrsim \frac{6 \times 0.25/2.49}{2.5 - \dfrac{3}{2.49}}$$

$$\gtrsim 0.465 \text{ cm}$$

Thickness needed for low-energy collimators are only a few tenths of a millimeter, which is in the range of lead "foil" thicknesses and approaches the limits of lead thicknesses that can be used without loss of necessary mechanical strength. Indeed, low-energy collimators generally are quite fragile, and their septa can be damaged easily by mechanical abuse (dropping, stacking on sharp objects, etc.). Medium-energy collimators require substantially greater thicknesses, typically a few millimeters of lead.

Low-energy γ-ray emiters (e.g., ^{99m}Tc, 140 keV) can be imaged using medium-energy collimators. This is done, however, with an unnecessary sacrifice of collimator efficiency because the collimator septa are unnecessarily thick. (See Table 16-2 for comparative efficiencies of low- and medium-energy collimators.) Low-energy collimators are used whenever possible to obtain maximum collimator efficiency. When choosing a collimator, however, one must consider not only the energy of the γ rays to be imaged but also the energies of any other γ rays emitted by the radionuclide of interest or by other radionuclides that may be present as well, e.g., residual activity from another study or radionuclide impurities. Higher-energy γ rays may be recorded by Compton downscatter into a lower-energy analyzer window. If the collimator septa are too thin, the collimator may be virtually transparent to higher-energy γ rays, causing a relatively intense "foggy" background image to be superimposed on the desired image, with a resulting loss of image contrast. Whether or not a low-energy collimator can be used when higher-energy γ rays are present depends on the energy and intensity of those emissions and requires experimental evaluation in specific cases.

3. Geometry of Collimator Holes

Collimator performance also is affected by the geometry of the collimator holes, specifically, their *shape, length*, and *diameter*.

The preferred hole shape, to maximize the exposed area of detector surface for a given septal thickness, is round or hexagonal, with the holes arranged in a close-packed hexagonal array. Square and triangular holes also have been used.

Collimator hole length and diameter affect strongly both collimator resolution and collimator efficiency. Collimator resolution R_c is defined as the full width at half-maximum (FWHM) of the radiation profile from a point or line source of radiation projected by the collimator onto the detector (Figure 16-12). This profile is also called the *point* or *line spread function* (PSF or LSF). Collimator resolution R_c is given by†

$$R_c \approx d(l_e + b)/l_e \tag{16-6}$$

where b is the distance from the radiation source to the collimator, and d is the diameter and $l_e = l - 2\mu^{-1}$ the "effective length" of the collimator holes (Figure 16-12). Here μ is the linear attenuation coefficient of the collimator material. The effective length of the collimator holes is somewhat less than their actual length due to septal penetration. From Example 16-1 it can be seen that for low-energy collimators (150 keV), the difference between effective and actual length is about 0.1 cm whereas for medium-energy collimators it is about 0.8 cm.

† It should be noted that some versions of Equation 16-6 include additional correction terms involving the thickness of the detector crystal, reflecting the fact that the image actually is formed at some depth within the detector crystal. Because photons of different energies penetrate to different average depths within the crystal, the correction actually is photon-energy dependent, a point not noted by most authors. The correction is small and for simplicity is omitted from Equation 16-6, as well as from Equations 16-10 and 16-13 for the converging and diverging collimators presented later in this chapter.

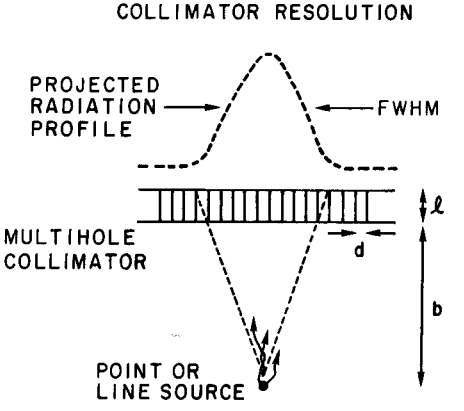

Fig. 16-12. Radiation profile (point or line spread function, PSF or LSF) for a parallel-hole collimator. The FWHM (full width at half-maximum) of the profile is used to characterize collimator resolution.

Example 16-2.
Calculate the resolution (FWHM) of the low-energy collimator described in Example 16-1, at source depths $b = 0$ and $b = 10$ cm, assuming it has a septal thickness of 0.03 cm.

Answer.
The effective length of the collimator is

$$l_e = 2.5 \text{ cm} - (2/21.43) \text{ cm}$$
$$\approx 2.4 \text{ cm}$$

Thus, for $b = 0$

$$R_c \approx 0.25(2.4 + 0)/2.4 \text{ cm}$$
$$\approx 0.25 \text{ cm}$$

and at $b = 10$ cm

$$R_c \approx 0.25(2.4 + 10)/2.4 \text{ cm}$$
$$\approx 1.3 \text{ cm}$$

This example illustrates the strong dependence of collimator resolution on source distance from the collimator.

Collimator efficiency g, defined as the fraction of γ rays passing through the collimator per γ ray emitted by the source, is given by

$$g \approx K^2(d/l_e)^2[d^2/(d + t)^2] \tag{16-7}$$

where t is septal thickness and K is a constant that depends on hole shape ($\sim$0.24 for round holes in a hexagonal array, $\sim$0.26 for hexagonal holes in a hexagonal array, $\sim$0.28 for square holes in a square array)[1]

Equation 16-7 applies to a source *in air* and assumes no attenuation of radiation by intervening body tissues.

Several aspects of Equations 16-6 and 16-7 should be noted. First, resolution improves as the ratio of hole diameter to effective length (d/l_e') is made smaller. Long, narrow holes provide image with the best resolution; however, collimator efficiency decreases approximately as the *square* of the ratio of hole diameter to length, $(d/l_e')^2$. Thus an approximate relationship between collimator resolution R_c and efficiency g is

$$g \propto R_c^2 \tag{16-8}$$

Example 16-3.

Calculate the efficiency g of the collimator described in Examples 16-1 and 16-2, assuming it has hexagonal holes in an hexagonal array.

Answer.

For hexagonal holes in a hexagonal array, $K = 0.26$

$$g \approx (0.26)^2\,(0.25/2.4)^2\,[(0.25)^2 / (0.25 + 0.03)^2]$$

$$\approx (0.0676) \times (0.0109) \times (0.797)$$

$$\approx 5.85 \times 10^{-4} \text{ (photons transmitted/photons emitted)}$$

This example illustrates the relatively small fraction of emitted γ rays that are transmitted by a typical Anger camera collimator.

Therefore, for a given septal thickness, collimator resolution is improved only at the expense of decreased collimator efficiency, and vice versa. The implications of this important tradeoff in collimator design are discussed further in Chapter 18, Section C.2.

Equation 16-7 also demonstrates the effect of septal thickness on efficiency. As noted in Section B.1, medium-energy collimators have lower efficiencies than low-energy collimators because of their greater septal thicknesses.

In addition to providing low- and medium-energy collimators, manufacturers of Anger camera systems also provide a selection of collimators with different combinations of resolution and efficiency. Those with good resolution but poor efficiency generally are described as "high resolution" collimators, whereas those with the opposite characteristics are described as "high sensitivity" collimators. Those with characteristics intermediate to the extremes are referred to as "general purpose," "all purpose," or by other similar names.

Equation 16-6 indicates that collimator resolution becomes poorer as source-to-collimator distance b increases. Thus structures closest to the collimator are imaged with sharpest detail. Figure 16-13 shows graphically the relationship between collimator resolution and source-to-collimator distance for three different collimators provided by one commercial manufacturer. Typically, collimator resolution deteriorates by a factor of 2 at a distance of 4–5 cm from the collimator.

On the other hand, according to Equation 16-7, collimator efficiency for a source in air is independent of source-to-collimator distance b. This rather surprising result is obtained provided the counting rate for the

entire detector area is measured. The reason for this is illustrated by Figure 16-14. As the source is moved farther away from the collimator, the efficiency with which radiation is transmitted through any one collimator hole decreases in proportion to $1/b^2$ (inverse-square law), but the number of holes through which radiation can pass to reach the detector increases in proportion to b^2. The two effects cancel each other, with the result that total counting rate—and thus collimator efficiency—does not change with source-to-collimator distance. Another illustration of this effect is shown in Figure 16-15. As source-to-collimator distance increases, the maximum height of the PSF or LSF decreases, but the width increases (and resolution becomes poorer), so that the total area under the curve (total detector counting rate) does not change.

Invariance of collimator efficiency with source-to-collimator distance applies to point sources, line sources, and uniform sheet sources in air with parallel-hole collimators; however, it applies only to uniform sheet sources with converging, diverging, or pinhole collimators (Section C). When the source is embedded at different depths in the patient, attenuation effects also must be considered. Septal penetration and scatter of photons from the walls of the collimator holes also are not considered in the above analysis.

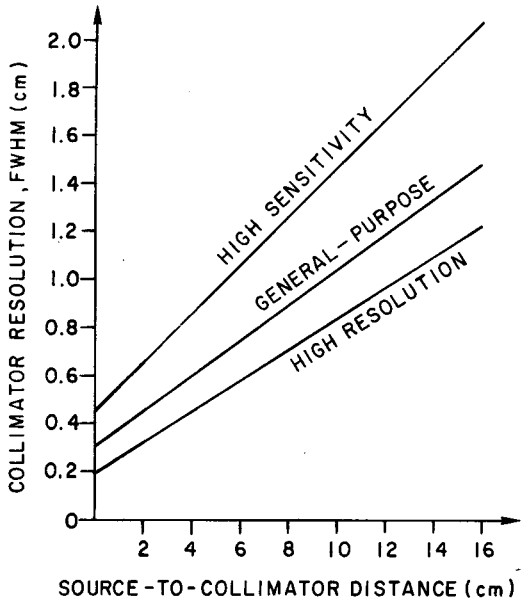

Fig. 16-13. Collimator resolution versus source-to-collimator distance for three different collimators. [Adapted from ref. 4: Hine GJ, Paras D, Warr CP: Recent advances in gamma-camera imaging. Proc SPIE 152:123, 1978, permis-

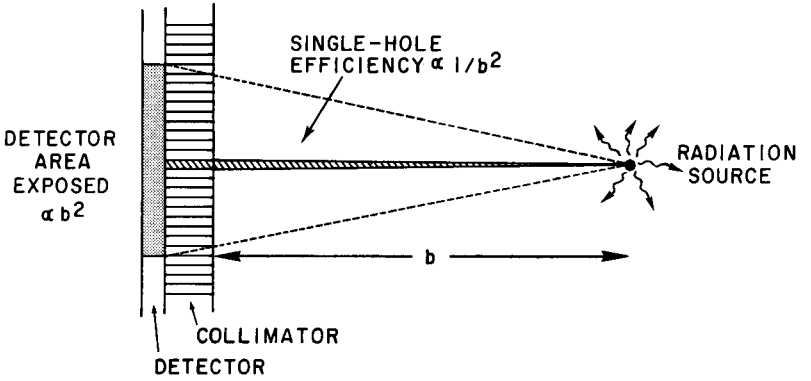

Fig. 16-14. Explanation for constant counting rate (collimator efficiency) versus source-to-collimator distance for a point source in air and a parallel-hole collimator. Efficiency for a single hole decreases as $1/b^2$, but number of holes passing radiation (area of detector exposed) increases as b^2.

Table 16-2 summarizes the performance characteristics of a number of collimators provided by one commercial manufacturer. Collimator resolution is the FWHM for a source at 10 cm from the face of the collimator. Collimator efficiency g refers to the relative number of γ rays transmitted by the collimator per γ ray emitted by the source. Note that the approximate relationship between collimator efficiency and resolution

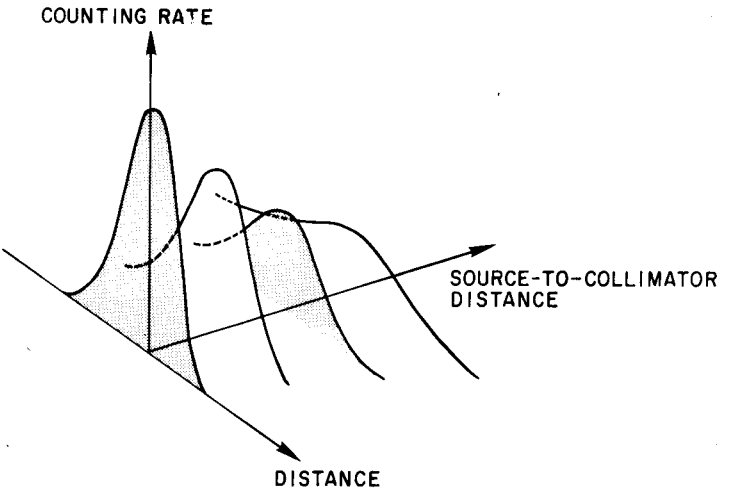

Fig. 16-15. Point spread functions versus distance for a parallel-hole collimator. Area under curve is proportional to collimator efficiency and does not change with distance.

given by Equation 16-8 is verified by these data. Note also the relatively small values of collimator efficiency.

4. System Resolution

The sharpness of images recorded with an Anger camera is limited by several factors, including intrinsic resolution, collimator resolution, scattered radiation, and septal penetration. In terms of the FWHM of a point or line spread function, the most important factors are the intrinsic resolution R_i of the detector and electronics and the collimator resolution R_c. The combined effect of these two factors is to produce a *system resolution* R_s that is somewhat worse than either one alone. System resolution R_s (FWHM) is given by

$$R_s = \sqrt{R_i^2 + R_c^2} \tag{16-9}$$

Because collimator resolution depends on source-to-collimator distance, system resolution also depends on this parameter. Figure 16-16 shows system resolution versus source-to-collimator distance for a typical parallel-hole collimator and different values of intrinsic resolution. At a distance of 5–10 cm (typical depth of organs inside the body), *system resolution* is much poorer than intrinsic resolution and is determined primarily by *collimator resolution*. There are significant differences between system resolutions for cameras having substantially different intrinsic resolutions (e.g., 4 mm versus 8 mm), but the difference in system resolutions for cameras having small differences in intrinsic resolutions (e.g., 4 mm versus 5 mm) is minor and not clinically

Table 16-2
Performance Characteristics of Some Typical Commercially Manufactured Parallel-Hole Collimators

Collimator Type	Suggested Maximum Energy (keV)	Efficiency g	Resolution R (FWHM at 10 cm)
Low energy, high resolution	150	1.84×10^{-4}	7.4 mm
Low energy, general purpose	150	2.68×10^{-4}	9.1 mm
Low energy, high sensitivity	150	5.74×10^{-4}	13.2 mm
Medium energy, high sensitivity	400	1.72×10^{-4}	13.4 mm

Adapted from ref. 3: Hine GJ, Erickson JJ: Advances in scintigraphic instruments, in Hine GJ, Sorenson JA (eds): Instrumentation in Nuclear Medicine (vol 2). New York,

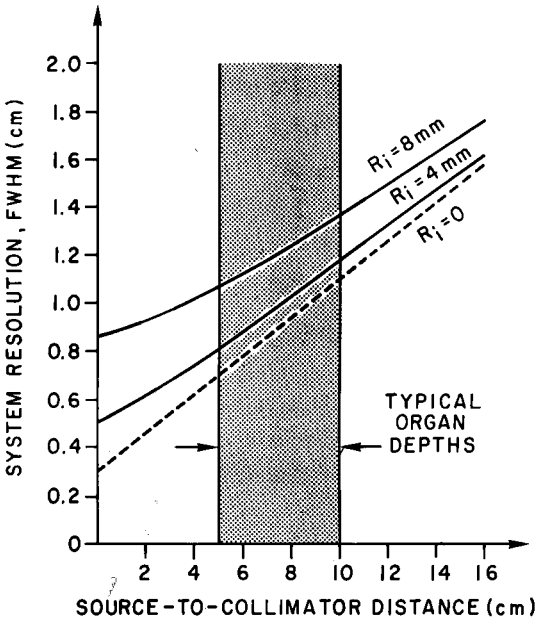

Fig. 16-16. System resolution versus source-to-collimator distance for a typical parallel-hole collimator and for different values of intrinsic resolution. At most typical organ depths, system resolution is determined primarily by collimator resolution.

significant. Small differences in intrinsic resolution may be apparent on bar pattern images or on images of very superficial structures in the patient, but they usually are not apparent on images of deeper-lying structures.

System resolution also is degraded by scattered radiation. This is discussed in Chapter 18, Section B. The method for combining component resolutions to determine system resolution also is discussed in Appendix G.

C. PERFORMANCE CHARACTERISTICS OF CONVERGING, DIVERGING, AND PINHOLE COLLIMATORS

Equations for collimator resolution, R_c, and efficiency, g, for converging, diverging and pinhole collimators are as follows:

CONVERGING COLLIMATOR

$$R_c \approx [d(l'_e + b)/l'_e][1/\cos\theta][1 - (l'_e/2)/(f + l'_e)] \quad (16\text{-}10)$$

$$g \approx K^2(d/l'_e)^2[d^2/(d + t)^2][f^2/(f - b)^2] \quad (16\text{-}11)$$

$$l'_e \approx (l - 2\mu^{-1})/\cos\theta \quad (16\text{-}12)$$

DIVERGING COLLIMATOR

$$R_c \approx [d(l'_e + b)/l'_e][1/\cos\theta][1 + (l'_e/2f)] \quad (16\text{-}13)$$

$$g \approx K^2(d/l'e)^2[d^2/(d + t)^2][f + l)/(f + l + b)] \quad (16\text{-}14)$$

PINHOLE COLLIMATOR

$$R_c \approx d_e(l + b)/l \quad (16\text{-}15)$$

$$g \approx d_e \cos^3\theta/16b^2 \quad (16\text{-}16)$$

$$d_e = \sqrt{d[d + 2\mu^{-1}\tan(\alpha/2)]} \quad (16\text{-}17)$$

The parameters in these equations are as shown in Figure 16-17. For the pinhole collimator, d_e is the "effective" pinhole diameter, accounting for penetration of the edges of the pinhole aperture. The equations for collimator resolution R_c refer to the equivalent FWHM of the point- or

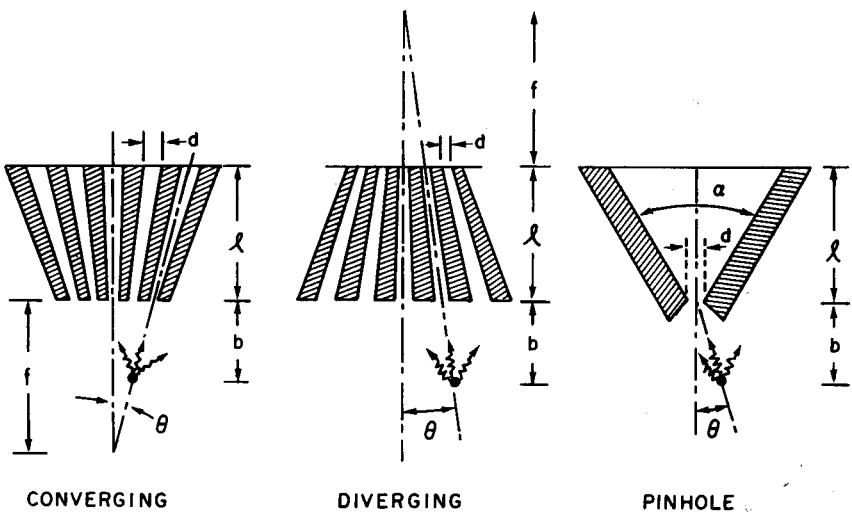

Fig. 16-17. Parameters for collimator resolution, R (FWHM), and efficiency, g (transmitted/emitted photons), for Equations (16-17). Adapted with permission from Medical Physics Data Book, Padikal TN, Fivozinsky SP (eds). Washington DC, National Bureau of Standards, 1982, pp. 48–55.

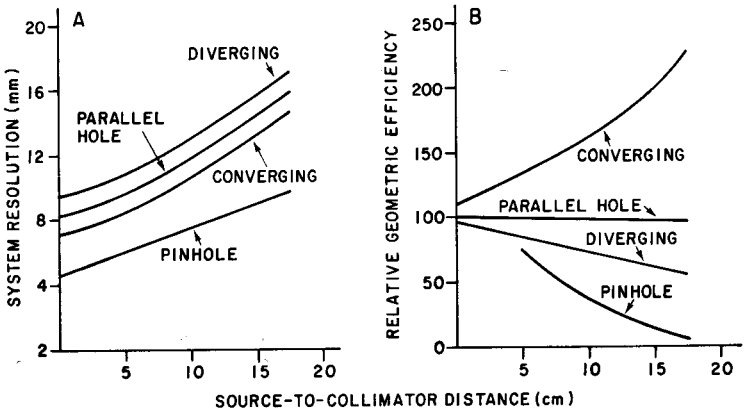

Fig. 16-18. Performance characteristics (left, system resolution; right, point-source geometric efficiency in air) versus source-to-collimator distance for four different types of Anger camera collimators. [From Rollo FD, Harris CC: Factors affecting image formation, in Rollo FD (ed): Nuclear Medicine Physics, Instrumentation, and Agents. St. Louis, C.V. Mosby Co., 1977. Modified from Moyer RA: J Nucl. Med. *15*:59, 1974].

line-source spread function, corrected for magnification or minification of the image by the collimator (Equations 15-3, 15-5, and 15-6). Thus, if the collimator projects a profile with a 2 cm FWHM measured on the detector and the image magnification factor is $\times 2$, the equivalent FWHM in the imaged plane is 1 cm.

The equations above may be compared with Equations 16-6 and 16-7 for parallel-hole collimator. They are similar except for the presence of additional terms involving collimator focal lengths f and, for off-axis sources, the angle θ between the source, the focal point (or pinhole), and the central axis of the collimator (Figure 16-7). The equations illustrate that for converging and diverging collimators, resolution is best at the center ($\theta = 0$, $\cos \theta = 1$).

The performance characteristics of different types of collimators are compared in Figure 16-18 which shows *system* resolution and efficiency vs. distance, including effects of camera intrinsic resolution as well as collimator magnification. Figure 16-18 illustrates that resolution always is best with the source as close as possible to the collimator. Changes in collimator efficiency with distance depend on whether the radiation source is a point source or a uniform sheet source. For a point source (Figure 16-18, right), collimator efficiency increases with increasing source-to-collimator distance with the converging collimator. Maximum efficiency is obtained at the collimator convergence point (~35 cm), where γ rays are transmitted through all of the collimator holes, and then

decreases beyond that point. Point-source collimator efficiency decreases with distance for the diverging and pinhole collimators, more severely for the latter. For an extended, large-area sheet source, sufficiently large to cover the entire field of view of the collimator, efficiency does not change with source-to-collimator distance for all of these collimators. Again, for sources embedded within a patient, attenuation effects also must be accounted for.

Figure 16-18 illustrates that the converging collimator offers the best combination of resolution and efficiency at typical imaging distances (5–10 cm); however, the field of view is also somewhat limited at these distances (Equation 15-6, Example 15-2), and for this reason converging collimators are most useful with cameras having relatively large area detectors. Diverging collimators offer a larger imaging area (Example 15-1) but at the cost of both resolution and efficiency. Pinhole collimators offer very good resolution and reasonable efficiency at close distances but lose efficiency very rapidly with distance; they also have a quite limited field of view because of magnification effects at typical imaging distances (Equation 15-3). Generally they are used for imaging smaller organs that can be positioned close to the collimator, e.g., thyroid and heart. They also are useful with high-energy γ-ray emitters because they do not suffer from septal penetration problems.

Differences between the resolution and field of view obtained at different source-to-collimator distances with parallel-hole, converging, diverging, and pinhole collimators are further illustrated by Figure 16-19.

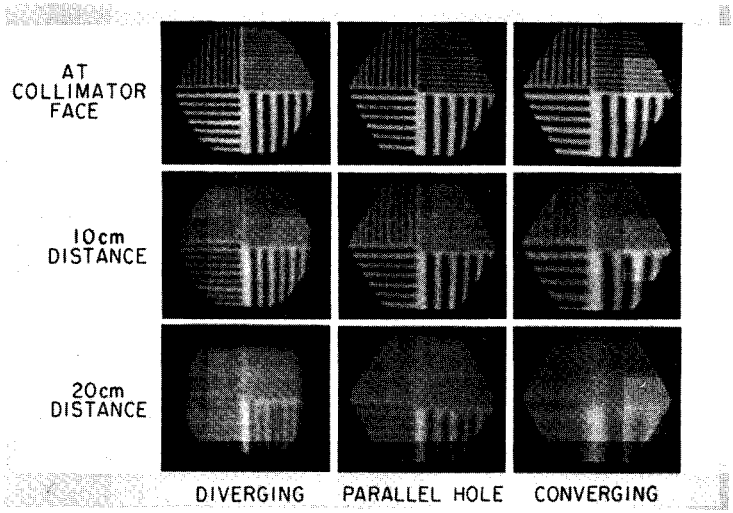

Fig. 16-19. Bar pattern images demonstrating changing field size and resolution obtained vs. distance for three collimator types.

It should also be noted that the distortions caused by changing magnification with depth for different structures inside the body sometimes make images obtained with the converging, diverging, and pinhole collimators difficult to interpret (see Figure 15-8).

REFERENCES

1. Anger HO: Radioisotope cameras, in Hine GJ (ed): Instrumentation in Nuclear Medicine (vol 1). New York, Academic Press, 1967, chap 19
2. Strand S-E, Larsson I: Image artifacts at high photon fluence rates in single-crystal NaI(Tl) scintillation cameras. J Nucl Med 19:407–413, 1978
3. Hine GJ, Erickson JJ: Advances in scintigraphic instruments, in Hine GJ, Sorenson JA (eds): Instrumentation in Nuclear Medicine (vol 2). New York, Academic Press, 1974, chap 1
4. Hine GJ, Paras D, Warr CP: Recent advances in gamma-camera imaging. Proc SPIE 152:121–126, 1978

Additional discussions of Anger camera performance characteristics and collimator design are discussed in the following:

Hine GJ, Paras P, Warr CP: Measurement of the Performance Parameters of Gamma Cameras, Part I. Rockville, MD., U.S. Dept. H.E.W., Publ. No. (FDA)78-8049, 1977

Richardson RL: Anger scintillation camera, in Rollo FD (ed): Nuclear Medicine Physics, Instrumentation, and Agents. St. Louis, C.V. Mosby Co., 1977, chap 6